EMINESCU AND THE TRANSITION TO PEAK-RING BASINS ON MERCURY. S. C. Schon,[1] J. W. Head,[1] L. M. Prockter[2], and the MESSENGER Science Team.[3] [1]Dept. of Geological Sciences, Brown University, Providence, RI 02906 USA; [2]JHU/APL, Laurel, MD; [3]http://messenger.jhuapl.edu/who_we_are/science_team.html.

Introduction: The MESSENGER [1] flybys have yielded a range of new scientific findings for Mercury [2] including evidence of embayment relationships indicative of volcanic plains activity [3,4] and an improved size estimate for the Caloris basin [5]. These new data reveal a broad continuum of Mercurian crater morphologies [6] in greater detail than prior studies that relied on Mariner 10 or Earth-based radar observations [7]. This study focuses on mapping the interior deposits of Eminescu, a central peak-ring basin, and is part of a larger comparative analysis of transitional crater morphologies observed on Mercury and the Moon in new data sets [8].

Impacts on Mercury occur at much higher velocities than lunar impacts and correspondingly generate more impact melt. Cintala [9] estimated that for a given projectile, the velocity difference will lead to twice as much impact melt on Mercury than on the Moon. Here we examine images at ~150 m/pixel resolution of the fresh impact crater Eminescu to document the nature of fresh crater interiors on Mercury at the transition from complex to peak-ring morphology. We also consider the importance of impact melt, and potentially volcanism, as processes responsible for albedo contrasts observed in the floor materials (Fig. 1).

Observations: Eminescu, approximately 125 km in diameter, is in the "mature-complex crater" class (30 < diameter (D) < 160 km) characterized by terraces and central peak elements in the morphological classification scheme of Pike [6]. Eminescu is intriguing because it has sharp albedo contrasts between floor units and the central peak ring. The good preservation of these features makes Eminescu a type-example of the transition from singular central peaks to central peak rings. The crater has a continuous ejecta deposit that extends about one crater radius from the rim. Chains of secondary craters are observed radial to Eminescu, but no bright rays are observed; rather, nearby rays are associated with Xiao Zhao crater.

Crater Rim and Walls. The rim of Eminescu is uplifted, and the crater walls are modified by significant slumping that extends inward about 0.2 crater radii. Mapping of slump block contacts (red lines, Fig. 2) shows that between three and five major faults are observed in most sections of the crater wall. Most craters of this size have well-developed terraces, while minor wall failure and associated slump deposits are associated with the smaller class of immature-complex craters (9.5 < D < 29.1 km) [6].

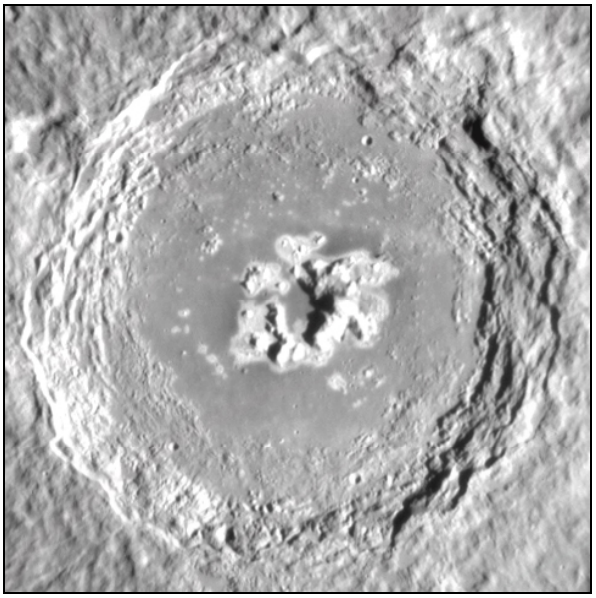

Figure 1: Eminescu Crater, ~125-km in diameter (10.8°N, 114.1°E), imaged during the first MESSENGER flyby.

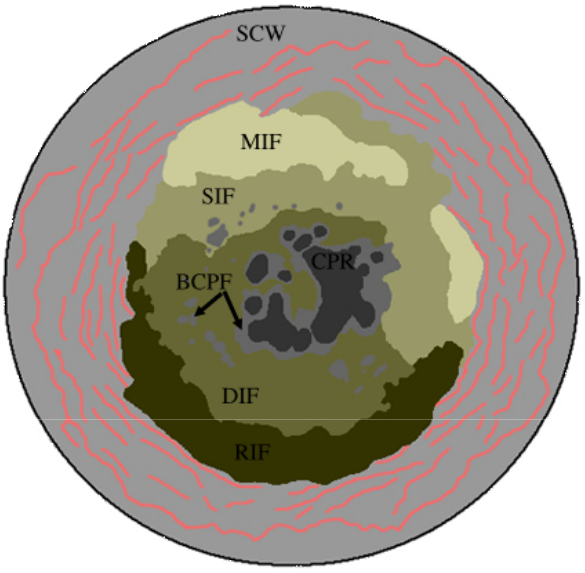

Figure 2: Geologic mapping of Eminescu crater interior. Full description in text: slumped crater wall (SCW), mottled interior facies (MIF), smooth interior facies (SIF), bright central peak facies (BCPF), central peak ring (CPR), dark interior facies (DIF), and rough interior facies (RIF).

Central Peak Ring. Eminescu has a pronounced high-albedo central peak ring (CPR). The uplifted peaks form a discontinuous ring. Dark smooth floor deposits occur both inside and outside the central peak ring. Surrounding the individual peak ring massifs are

large coalescent annuli of bright material (bright central peak facies, BCPF). This bright material follows the contours of the peak ring topography and borders the interior of the peak ring topography as well. The bright annuli could be the result of either: (1) material shed from the central peak massifs forming talus margins, or (2) embayment of autochthonous central peak bright material by the dark unit.

Crater Floor. The floor of Eminescu is subdivided into four units on the basis of albedo and texture. The interior of the central peak ring (interior to the bright annuli) is a smooth low-albedo unit (dark interior facies, DIF) that is continuous with dark smooth material flooring the central portion of the crater. The DIF unit has a sharp contact with the lower-albedo smooth unit (smooth interior facies, SIF). Both the DIF and SIF units have small circular/quasi-circular features of higher albedo and positive topography within them, similar to the central peak ring features that are mapped as BCPF; contacts between these features and the surrounding materials are also sharp. Farther from the crater center are mottled and rougher surface textures that comprise the mottled interior facies (MIF) and rough interior facies (RIF) units. These hummocky units contain interspersed regions of smooth texture (more in MIF than RIF) that are similar in appearance to ponded impact melt associated with lunar craters [10]. The MIF and RIF units are similar in albedo to the SIF unit.

Multispectral color data from MESSENGER's wide-angle camera was used [11] to define three primary spectral units: low-reflectance material, moderate- to high-reflectance smooth plains, and a spectrally intermediate unit. The heavily cratered region where Eminescu is located is the spectrally intermediate terrain. Three additional spectral units with limited extents are recognized: fresh crater ejecta, bright crater-floor deposits (BCFDs), and moderately high-reflectance reddish material [11, 12, 13]. The BCFD spectral unit corresponds the BCPF unit mapped in this study. Spectrally similar material is found in the central peak ring of Raditladi and is distinctive from the other crater floor materials observed in these craters. Raditladi is a young 250-km-diameter basin, with a prominent central peak ring (~125-km diameter) and distinctive extensional graben [14]. Whereas Raditladi is interpreted as having formed at 1 Ga or more recently [4], crater size-frequency distributions (Fig. 3) indicate that Eminescu is even younger.

Preliminary Conclusions: Two hypotheses may explain the origin of the smooth interior floor units and their relations to the central peak ring: (1) impact melt followed by slumping of material from the central peak ring massifs, or (2) impact-related volcanism that embayed the central peak ring. The bright annuli (extending for at least several kilometers) surrounding the central peaks are significantly more extensive than talus associated with lunar central peaks (e.g., Tycho), suggesting that embayment by the dark interior unit may be more plausible; however, no volcanic vent structures have been identified. The bright smooth interior unit (SIF) is similar in albedo to ponded deposits we interpret to be impact melt that are found in the mottled unit (MIF), but the SIF has higher albedo than the dark interior unit, also suggesting that the dark unit may be a superposing volcanic unit which has embayed the central peak ring, or a result of greater impact melt generation in Mercurian craters at the onset of central peak rings [e.g., 15]. Similar relations are observed in Raditladi; hypotheses will need to account for the observations in both craters, and be compatible with their young geologic ages. Observation with the full MESSENGER instrument suite during the primary mission will provide additional data to test and refine these hypotheses.

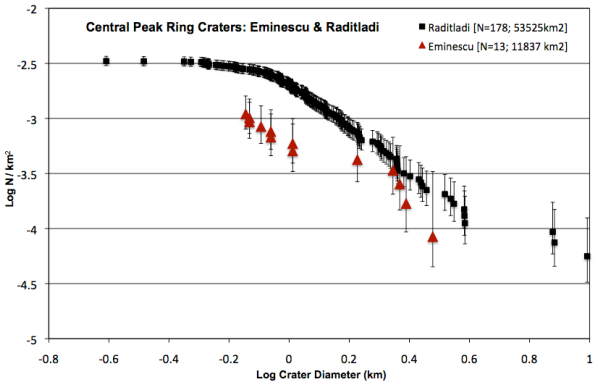

Figure 3: Crater size-frequency distributions for Eminescu and Raditladi. Raditladi's age is interpreted to be ~1 Ga [4]; Eminescu is resolvably younger.

References: [1] Solomon, S. C. et al. (2001), PSS 49, 1445-1465. [2] Solomon, S. C. et al. (2008) Science 321, 59-62. [3] Head, J. W. et al. (2008), Science 321, 69-72. [4] Strom, R. G. et al. (2008), Science 321, 79-81. [5] Murchie, S. L. et al. (2008), Science 321, 73-76. [6] Pike, R. J. (1988), in *Mercury*, F. Vilas et al. (eds.), pp. 165-273. [7] Head, J. W. et al. (2007), Space Sci. Rev. 131, 41-84. [8] Head, J. W. (2010) GRL, submitted. [9] Cintala, M. J. (1992), JGR 97, 947–973. [10] Hawke, B. R. and J. W. Head (1976), Symp. Planet. Cratering Mechanics, LPI, pp. 44-46. [11] Robinson, M. S. et al. (2008) Science 321, 66-69. [12] Blewett, D. T. et al. (2009), EPSL 285, 272-282. [13] Blewett, D. T. et al. (2010) Icarus, in press. [14] Prockter, L. M. et al. (2009) LPS 40, #1758. [15] Cintala, M. J. and R. A. F. Grieve (1998) MAPS 33, 889-912.